JPE 16-4-24

http://dx.doi.org/10.6113/JPE.2016.16.4.1494
ISSN(Print): 1598-2092 / ISSN(Online): 2093-4718

Parallel-Connected Magnetic Energy Recovery Switch Used as a Continuous Reactive Power Controller

Yewen Wei[*,**], Bo Fang[***], Longyun Kang[†], Zhizhen Huang[**], and Teguo liu[****]

[*]College of Electrical Engineering & New Energy, China Three Gorges University, Yichang, China
[**,†]New Energy Research Center of Electric Power College, South China University of Technology, Guangzhou, China
[***]Electrical & Mechanical College, Xuchang Uiversity, Xuchang, China
[****] Dongguan Power Supply Bureau, Guangdong Power Grid Corporation, Dongguan, China

Abstract

Power quality promotion has received increasing attention because of the wide use of semiconductor devices in recent decades. Reactive power regulation is crucial to ensuring the stable operation of power systems. In this study, a continuous reactive power controller, which is referred to as a parallel-connected magnetic energy recovery switch (MERS), is developed to regulate voltage or power factor in power grids. First, the operating principle is introduced, and a mathematical model is built. Second, a new control method for restraining current harmonics and the peak voltages of capacitors is presented. Using the proposed method, the MERS shows a wide range in terms of reactive power compensation. Finally, the performance of the proposed controller is demonstrated through computer simulations and experiments. Unlike STATCOMs, the proposed controller entails low losses, adopts a small dc capacitor, and offers ease of use.

Key words: Continuous reactive power controller, Parallel-connected magnetic energy recovery switch, Power factor correction, Power quality

I. INTRODUCTION

With the ever-increasing application of semiconductor devices in power systems, power quality tends to deteriorate because of power factor decline, voltage instability, and increased harmonics. In addition, the reliability of power grids gradually decreases because of the connection of distributed power supplies, such as wind or solar generation systems. Reactive power compensation technology, which is applied to correct the power factor or stabilize grid voltage, has been widely used to promote power quality [1]. Generally, a static var compensator (SVC) is usually installed near a load in a power system for PFC. The main types of SVC include thyristor switched capacitors (TSCs) [2], thyristor controlled reactors (TCRs), static synchronous compensators (STATCOMs) [3], and parallel-connected magnetic energy recovery switches (MERS) [4].

Unlike TSCs, TCR ssupply continuous inductive reactive power but not fixed capacitive reactive power. As high current harmonics are inserted into the grid, TCRs have been replaced with other SVCs. STATCOMs, which can supply continuous inductive reactive power and capacitive reactive power and produce low harmonics, have attracted significant attention in the area of power quality improvement [5]. However, this continuous reactive power controller always suffers from high frequency losses [6] and control method [7]. Some cascaded H-bridge STATCOMs exhibit a complex circuit structure and require additional current filters [8]. An emerging SVC called the MERS, which is used to supply continuous capacitive reactive power, was proposed about a decade ago. Its advantages include simple circuit structure,

Manuscript received Jul. 15, 2015; accepted Feb. 3, 2016
Recommended for publication by Associate Editor Kyo-Beum Lee.
[†]Corresponding Author: lykang@scut.edu.cn
Tel: +86-020-87111193,Fax: +86-020-87111193, South China Univ. of Tech.
[*]College of Electrical Engineering & New Energy, China Three Gorges University, China
[**]New Energy Research Center of Electric Power College, South China University of Technology, China
[***]Electrical & Mechanical College, Xuchang University, China
[****]Dongguan Power Supply Bureau, Guangdong Power Grid Corporation, China

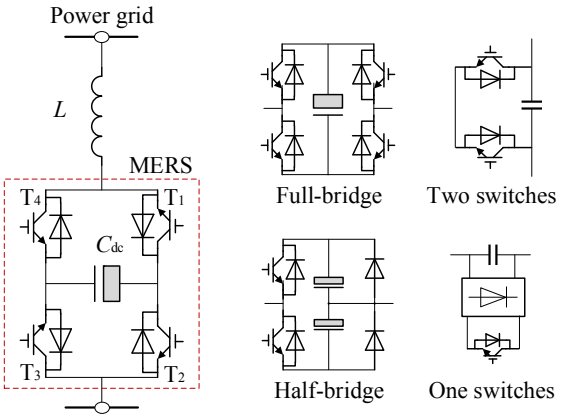

(a) MERS connected in parallel. (b) Four types of MERS.
Fig. 1. Circuit configuration of MERS.

line frequency control, low losses, and small capacitors [9] and [10].

MERS, which is used as a series compensator in [11] and [12], is connected to the power grid in parallel [13] as a shunt compensator, as shown in Fig. 1(a). Control methods based on a current phase are no longer suitable for shunt MERS because of the uncertainty of the grid current. After one switch is turned off in advance, the minimum voltage of a dc capacitor ($V_{C\text{-min}}$) is regulated [13]. This method can broaden the reactive power compensation range of MERS, but the distortion of the current waveform quickly increases. In addition, the large delay angle applied exceeds the high peak voltage of the dc capacitor ($V_{C\text{-peak}}$) and total harmonic distortion (THD) generated.

To improve the performance of a parallel-connected MERS, we first rebuild a mathematic model on the basis of the phase of the grid voltage.

Then, a new method adopting a cooperative control between parameters α and $V_{C\text{-min}}$ is proposed. The optimal control function and evaluation model are developed to optimize the effect of system control. A computer simulation and experiments are conducted, and the results support the conclusions. The proposed SVC and STATCOMs are also compared to expound the feasibility and advantages of the former.

II. Parallel-Connected Magnetic Energy Recovery Switch

This section introduces the theoretical analysis, including the circuit configuration and operating principle. According to the voltage and current waveforms of MERS, its mathematical model is rebuilt on the basis of the phase source voltage. Then, some disadvantages of the existing control are pointed out in detail.

A. Circuit Configuration

As described in the reference [12], a single MERS consists of four switches and a dc capacitor. Three MERSs are used in a three-phase system. Between the grid and the MERS, a small inductor needs to be connected when the SVC is installed. The parallel-connected MERS is shown in Fig. 1(a). Fig. 1(b) shows four types of MERS. Only the full-bridge MERS is considered in this study.

B. Operating Principle and Mathematical Model

The four switches of the full-bridge MERS are divided into two groups, namely T_1–T_3 and T_2–T_4. Every group is usually opened at the same time but is closed asynchronously. The states of different switches, which are determined by control parameters $V_{C\text{-min}}$ and α, can lead to different running modes. When $V_{C\text{-min}}$ and α are equal to zero, the mode is referred to as a balanced mode. The output reactive power (Q_{out}) of this mode is defined as Q_0. Increasing $V_{C\text{-min}}$ or α separately results in Q_{out} being lower or higher than Q_0, respectively. Using the control method proposed in [13] and taking the source voltage for reference, we obtain the current and voltage waveforms of the MERS, which are shown in Fig. 2. The two control styles [13] are presented in Figs. 2(a) and (b). The former one is under a dc off-set mode, and the latter one is under a discontinuous mode. In sum, $V_{C\text{-min}}$ control means changing the closing time, whereas α control means regulating the opening time.

The circuit of the shunt MERS can be simplified, as shown in Figs. 3(a) and (b), when the dc capacitor is bypassed or connected in series. R_{Line} is the equivalent resistance of the line, and ωt is the variable phase angle. u_s is the ac source voltage. Taking a single cycle for transient state analysis, we establish voltage balance equations on the basis of Kirchhoff's voltage law as follows:

(1) $\omega t \in [-\alpha, \alpha]$ or$[\pi-\alpha, \pi+\alpha]$

$$L\bullet(di_{MERS}/dt)+R_{line}i_{MERS}=U_m\sin\omega t \tag{1}$$

(2) $\omega t \in [\alpha, \pi-\alpha]$ or$[\pi+\alpha, 2\pi-\alpha]$

$$\begin{cases} L\bullet(di_{MERS}/dt)+R_{line}i_{MERS}+U_C=U_m\sin\omega t \\ U_C=\int i_{MERS}dt/(\omega C_{dc})+\mathrm{sgn}(\sin\omega t)\bullet V_{C\text{-min}} \end{cases} \tag{2}$$

Where U_m denotes the amplitude of u_s and ω is the angular speed ($\omega = 2\pi f$, f is the grid frequency). Sgn (x) is a signum function that outputs +1 if $x \geq 0$, else −1.

As Fig. 3 shows, the curves of V_{MERS} and i_{MERS} can be separately expressed with odd and even functions, respectively.

$$u_{MERS}(\omega t)=\sum_{n=1}^{\infty} b_n \sin n\omega t, \quad n=2N-1 \tag{3}$$

$$i_{MERS}(\omega t)=\sum_{k=1}^{\infty} I_{mk}\cos(k\bullet\omega t), k\in N \tag{4}$$

Where b_n and I_{mk} denote the amplitudes of each voltage and current harmonic component, respectively.

In addition, the MERS voltage can be formulated with a

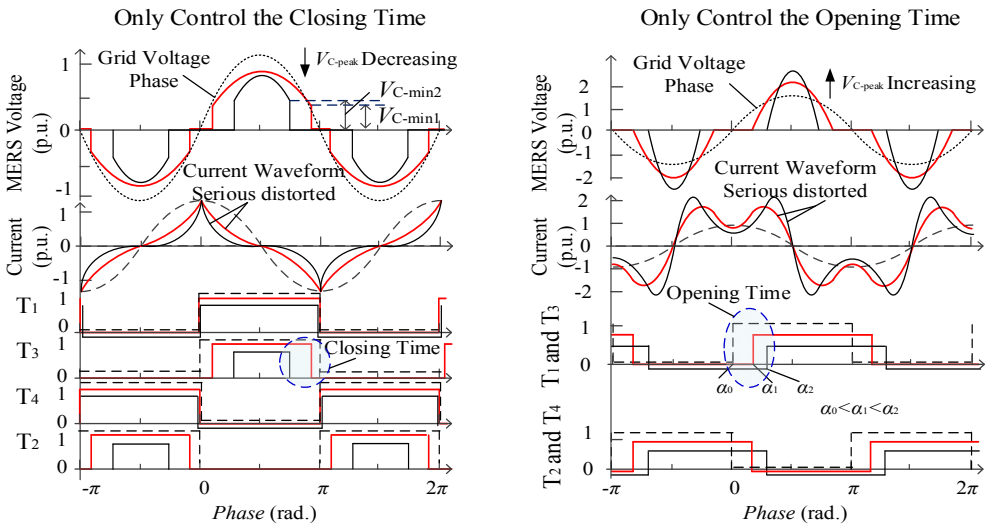

(a) $V_{C\text{-min}}$ control. (b) Delayed angle α control.

Fig. 2. Current and voltage waveforms using the existing control method.

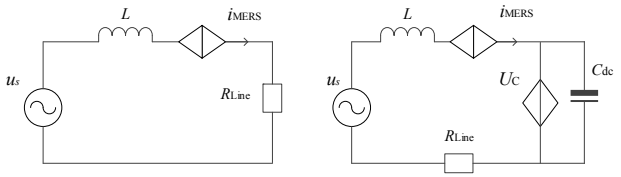

(a) With dc capacitor bypassed.(b) With dc capacitor connected.

Fig. 3. Simplified circuit when MERS runs in different modes.

piecewise function in the cycle from $-\alpha$ to $2\pi-\alpha$. In sum, u_{MERS} can be described by U_C, which is mentioned in equation (2). Then, the amplitude of the fundamental MERS voltage (b_1) is obtained by ignoring the high-order harmonics through the fast Fourier translation, as expressed in equation (5).

$$b_1 = \frac{4V_{C\text{-min}} \bullet \cos\alpha}{\pi} + \frac{\sqrt{2}I_{m1}}{\omega C_{dc}} \bullet \left[1 - \frac{2\alpha}{\pi} - \frac{\sin(2\alpha)}{\pi}\right] + B^* \quad (5)$$

Where I_{m1} is the amplitude of the fundamental MERS current. B^* is a high-order component.

By substituting equations (3) and (4) into equation (2), we can obtain the relationship between b_1 and I_{m1}while ignoring the high-order harmonics, as shown in equation (6).

$$b_1 = U_m + \omega L I_{m1} \quad (6)$$

For the dc off-set mode, α is set to zero, similar to $V_{C\text{-min}}$, which is fixed to zero under the discontinuous mode. With equations (5) and (6), I_{m1} can be solved. According to Ohm's law, the equivalent capacitances of the dc off-set and discontinuous modes are described in equation (7).

$$X_{MERS} = \begin{cases} \dfrac{\pi U_m - 2\sqrt{2}DV_{C\text{-min}}}{\pi U_m - 4V_{C\text{-min}}} \bullet X_{C_{dc}} + X_1^*, \text{ dc off-set mode} \\ \left[1 - \dfrac{(2\alpha + \sin 2\alpha)}{\pi}\right] \bullet X_{C_{dc}} + X_2^*, \text{ discontinous mode} \end{cases} \quad (7)$$

where $D = X_L/(\pi \bullet X_{Cdc})$ and X_1^* and X_2^* are high-order components that are generally ignored.

Then, $X_{P\text{-C MERS}}$ is deduced with equation (8).

$$X_{P\text{-C MERS}} = X_{MERS} - X_L \quad (8)$$

TABLE I

CONTROL EFFECT OF PARAMETERS VC-MIN AND A

	dc off-set mode: increasing $V_{C\text{-min}}$	discontinuous mode: increasing α
Q_{out}	↓	↑
$V_{C\text{-peak}}$	↓	↑
THD_i	↑	↑

Notes: "↓" means decreasing, and "↑" means increasing.

where P-C MERS denotes the parallel-connected MERS.

The model of Q_{out} as a novel compensator can be finally formulated as follows:

$$Q_{out} = U_m^2 / X_{P\text{-CMERS}} \quad (9)$$

C. Shortcomings to be Addressed

Theoretically, $X_{P\text{-C MERS}}$ can be regulated from 0 to infinity using equation (8). However, power quality severely declines that the range of control parameters $V_{C\text{-min}}$ or α becomes limited, as revealed in Fig. 2. Hence, Q_{out} must be controlled within a limited range. For instance, the output reactive power of MERS is not lower than $0.9Q_0$ and not higher than $1.4Q_0$ in reference [4]. As shown in Fig. 2, increasing α causes $V_{C\text{-peak}}$ to increase, and large $V_{C\text{-min}}$ and αcorrespond to a high current THD.

However, the curves presented on top of Fig. 2(a) show that increasing $V_{C\text{-min}}$ can cause $V_{C\text{-peak}}$ to decline. Thus, regulating this parameter could possibly decrease the peak voltage of the capacitor successfully. The triple harmonic is a major part of the MERS current, except for the fundamental harmonic under the discontinuous mode.

As α increases, the sinusoid current may be acquired if the triple harmonic is filtered [13]. This characteristic is specially fit for triangle-connected triple shunt MERSs in three-phase systems. The control effects of $V_{C\text{-min}}$ and α on

regulating Q_{out} and power quality arelisted in Table I. To promote the capability of the parallel-connected MERS in terms of CRP control, a considerably wide range of parameters $V_{C\text{-}min}$ and α should be applied when meeting the power quality requirements in the power grid. Therefore, a new control method is proposed in the present work by changing $V_{C\text{-}min}$ and α concurrently.

III. Performance Improvement Using Cooperative Control Parameters

To restrain current harmonics and $V_{C\text{-}peak}$, we first develop a type of cooperative control between parameters α and $V_{C\text{-}min}$. By establishing an optimal control function and an evaluation model, the system control strategy realizes perfect continuous reactive power tracking and reaches the best working points consistently.

A. Cooperative Control between Parameters α and VC-min

Using the same method as that deduced in equation (7), we build a new capacitance model when neither $V_{C\text{-}min}$ nor α is fixed to zero. The formulation is shown in equation (10). Then, equation (10) is substituted into equation (9), and a function of Q_{out} based on variable $V_{C\text{-}min}$ and α is obtained in equation (11).

$$X_{MERS}=\left[1-\frac{U_m(2\alpha+\sin 2\alpha)-(4-2\sqrt{2}D)V_{C\text{-}min}\bullet\cos\alpha}{\pi U_m-4V_{C\text{-}min}\bullet\cos\alpha}\right]\bullet X_{C_{dc}}+X^* \quad (10)$$

Where X^* is a high-order component.

$$Q_{out}=\frac{(\pi U_m-4V_{C\text{-}min}\bullet\cos\alpha)\omega C_{dc}U_m^2}{U_m(\pi\text{-}D\pi^2-2\alpha-\sin 2\alpha)+D(4\pi-2\sqrt{2})V_{C\text{-}min}\bullet\cos\alpha} \quad (11)$$

where X^* is extremely small and thus negligible.

Unlike that in the existing control method, the same Q_{out} is determined not with only one working point but with a series of working points, as shown in equation (11). These points comprise a line, which is called the equivalent reactive power line (ERPL). By taking the variable $V_{C\text{-}min}$ for the vertical axis and the variable α for the horizontal axis, we plot several ERPLs in a plane of rectangular coordinates, as shown in Fig. 4.

The simulation model is set up in PSIM as follows. Some points, which are marked as squares in Fig. 4, are measured to verify the existence of an ERPL via simulation. A waveform comparison between point-(25^0, 0V) and point-(28^0, 58V) is shown in Fig. 4. These two points generate the same Q_{out}, but point-(25^0, 0V) suffers from larger $V_{C\text{-}peak}$ and harmonics in comparison with point-(28^0, 58 V).

B. Optimal Control Function and Evaluation Model

Not all points are allowed on an ERPL. Some points with low current harmonics and $V_{C\text{-}peak}$, similar to the second point shown in Fig. 5, are the optimal ones sought in this work.

$V_{C\text{-}max}$ is defined as the maximum voltage to be endured by the capacitor and IGBTs. THD_{max}, with a triple harmonic

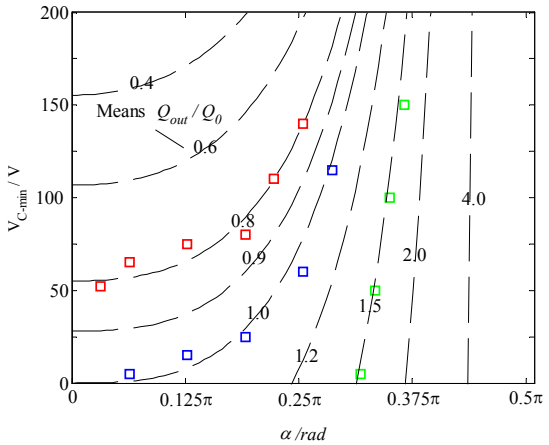

Fig. 4. ERPLs with the proposed control method.

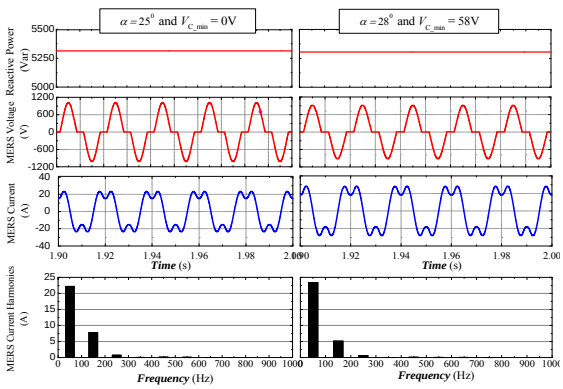

Fig.5. Waveform comparison when MERS supplies the same Q_{out}.

filtered in the MERS current, is defined as the maximum harmonic share to be accepted by the power grid. In the case of Q_{out}, $V_{C\text{-}min}$ can be expressed with a function, with αserving as the independent variable. Then, the optimal control function is established, as shown in equation (12). In ensuring the exact value of $V_{C\text{-}min}$ and α, the initial $V_{C\text{-}min}$ is always zero when Q_{out} is greater than Q_0. Conversely, the initial $\alpha$is equal to zero when $Q_{out}<Q_0$.

$$\begin{cases} V_{C\text{-}min}=\dfrac{\pi\omega C_{dc}U_m^2-Q_{out}(\pi\text{-}D\pi^2-2\alpha-\sin 2\alpha)}{[DQ_{out}(4\pi-2\sqrt{2})-4\omega C_{dc}U_m^2]\bullet\cos\alpha}\bullet U_m \\ THD_i<THD_{max} \quad \& \quad V_{C\text{-}peak}<V_{C\text{-}max} \end{cases} \quad (12)$$

To evaluate the performance of a chosen point, we develop a test function, which is shown in equation (13). A large F indicates that the currently working point performs satisfactorily. On the contrary, a low F indicates that a better working point should be selected.

$$F(THD_i,V_{C\text{-}peak})=100*\sqrt{(1-\lambda_{THD})\bullet(1.5-\lambda_{V_{C\text{-}peak}})} \quad (13)$$

Where λ_{THD} and $\lambda_{Vc\text{-}peak}$ are defined as follows:

$$\begin{cases} \lambda_{THD}=\mathrm{sgn}(1-\dfrac{THD_i}{THD_{max}})\bullet\dfrac{THD_i}{THD_{max}} \\ \lambda_{V_{C\text{-}peak}}=\mathrm{sgn}(1-\dfrac{V_{C\text{-}peak}}{V_{C-max}})\bullet\dfrac{V_{C\text{-}peak}}{V_{C-max}} \end{cases} \quad (14)$$

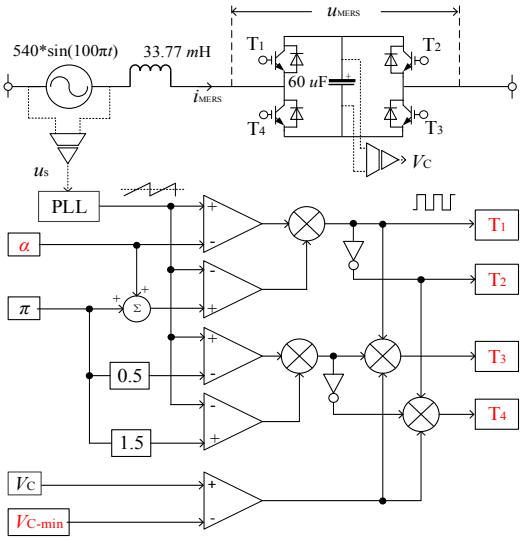

Fig. 6.Simulation model of single-phase shunt MERS.

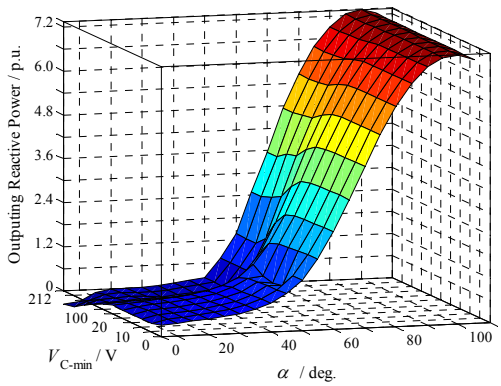

Fig. 7. Curve surface for describing the output reactive power.

C. Improved Performance with the Proposed Method

In PSIM, a simulation model is first set up. Its main system parameters are marked in Fig. 6, which also shows the logical process of control signal production. Using this model, we derive a curve surface on the basis of the simulation results shown in Fig. 7. This figure describes the output reactive power of MERS. Every Q_{out} corresponds to a plane that is parallel to the coordinate plane. A line intersecting a Q_{out} plane and the curve surface is an ERPL. Therefore, the range of working points is broadened and demonstrated.

As shown in Fig. 7, parameters $V_{C\text{-min}}$ and α show the same control effect as that presented in Table 1. When THD_{max} and $V_{C\text{-max}}$ are supplied, such as THD_{max} =6% and $V_{C\text{-max}}$ =1,000V, the improved power quality of MERS is revealed (Fig. 8). In Fig. 8, the dotted line denotes the current THD or $V_{C\text{-peak}}$ before the improvement with the control method. The THD of the MERS current shown in Fig. 8(a) does not include a triple harmonic. The left picture indicates that a large Q_{max} and a small Q_{min} are allowed after the improvement with the control method. Both types of output reactive power do not equate to current THD that exceeds the limited range. The rightmost picture supports a large Q_{out} while satisfying the highest peak voltage limit. Finally, the practical operating range of the novel CRPC is approximately expanded from $0.7Q_0$ to $3.0Q_0$. However, the output range after using the existing control method is only $0.9Q_0$–$1.4Q_0$. The performance of the developed method is clearly better than that of the existing method.

D. Control Strategy for Unit Power Factor Correction

To calculate the present power factor, we first track the phase difference between the grid voltage ψ_{GV} and current ψ_{GI}. Then, it is determined with equation (15). A PI controller is used to convert the error of the power factor to the changed reactive power ΔQ_{out}.

$$\lambda_{PF} = [0.5 - 0.5\,\mathrm{sgn}(\sin\Delta\psi_{GVI})] + \sin\Delta\psi_{GVI} \quad (15)$$

where $\Delta\psi_{GVI}$ is ψ_{GV}−ψ_{GI}.

To search for optimal control parameters, we adopt V_C and THD_i, as well as ΔQ_{out}, on the basis of equations (11) to (14). Furthermore, the output of an actual reactive power is derived from ΔQ_{out} and Q_{out} supplied by the previous cycle.

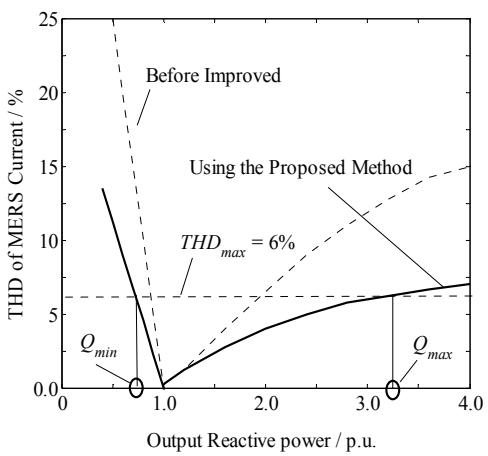

(a) Current THD without triple harmonic.

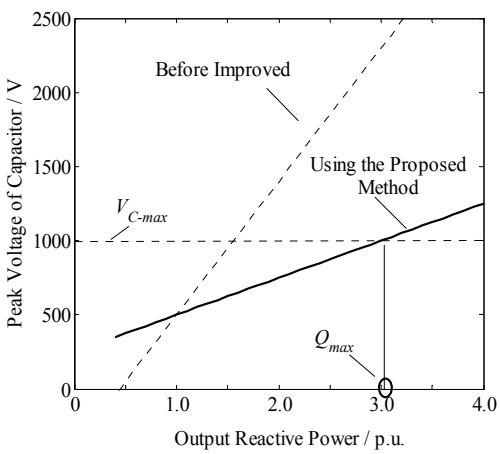

(b) Peak voltage of capacitor.

Fig. 8. Improved performance with the proposed control method.

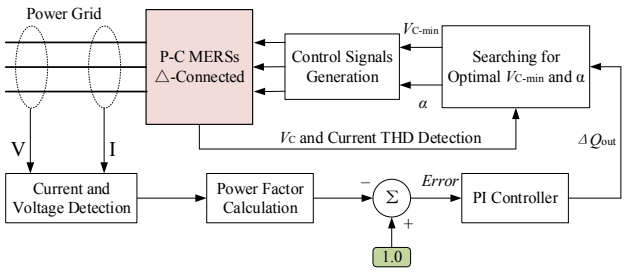

Fig. 9. Control strategy for three-phase parallel-connected MERS.

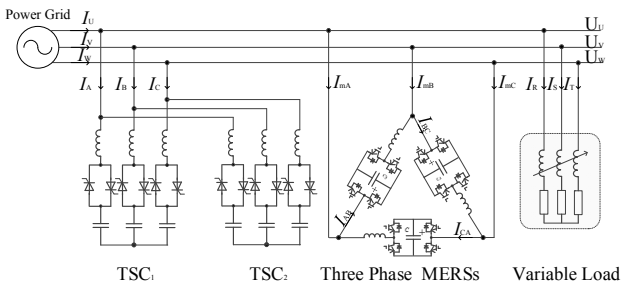

Fig. 10. Circuit structure for power factor correction system.

Finally, control signals are produced for the 12 switches in a three-phase MERS. Fig. 9 presents the process of power factor correction as analyzed above.

IV. Simulations and Experiments

A three-phase power system, which consists of an experimental MERS as well as variable loads and an ac source, is set up. The proposed control method is verified by simulations and experiments. The proposed system is compared with STATCOMs in terms of factors such as loss and soft switching. The results are then analyzed to explain the feasibility and advantages of the proposed system.

A. Experimental System

Fig. 10 shows the structure of the experimental system. The simulation model is set up in the same way as that in PSIM. It mainly includes MERS, TSC, and a variable load. TSCs are employed to support MERS in generating a large amount of reactive power. The circuit characteristics are listed in Table II.

An existing digital controller called Expert III is applied. This controller can run a self-designed program with a DSP C6713 integrated as its core chip. In addition, a special software called PE-View 9 is installed in a computer for managing the controller. The testing equipment includes TPS 2024 (200MHz), Fluke 43B Power Quality Analyzer, etc. We design a control program to realize the control strategy proposed in Fig. 9. Fig. 11 shows the working process.

B. Verification by Simulations and Experiments

A simulation is first completed to verify the transient response when the load changes. The performance of some working points represented by the function F is also measured. The transient response and steady-state characteristic are demonstrated through experiments.

TABLE II
System Specification for Simulation or Experimental Model

Three-phase grid voltage	380 V,50 Hz			
Current limiting reactor	33.77 *m*H×3			
Dc capacitor	60 *u*F×3			
CRPC range designed for MERS	2.2–7.66 kVar			
3.0 kVar TSC_1	L=11.1 *m*H	×3	C=61.33*u*F	×3
5.0 kVar TSC_2	L=22.0 *m*H	×3	C=132.3*u*F	×3
Variable load	50 *m*H<L < 150 *m*H; 3.0 Ω<R< 15.0 Ω			

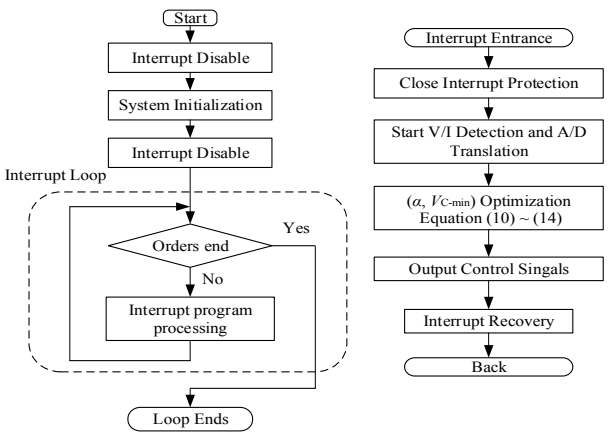

Fig. 11. Control program adopted in Expert III.

1) Simulation Verification: Fig. 12 shows the response of the power factor correction in the simulation when the load increases. The first change in load occurs at 5.6 s. The reactive power of the load increases from 7.0 kVar to 10 kVar. The grid power factor decreases obviously but reverts to a unit after about 0.05 s. In this recovery process, only TSC_1 is switched on, and MERS is left unchanged. The second change in load occurs at 5.8 s. TSC_2 is also applied, and the MERS current increases at the same time. The second recovery process takes about 0.04 s. The top part of Fig. 12 shows changes in grid power; the waveforms of the phase voltage and current are shown in the picture below the power grid.

The verification of the decrease in load is also completed, as shown in Fig. 13. The load changes twice at 9.62 and 9.86 s. The reactive power of the load decreases from 18 kVar to 10.0 kVar at the first period of change and from 10 kVar to 5.0 kVar at the second period of change. TSC_1 and $TSC_2$are cut off from the grid one by one. The shunt MERS works as a continuous reactive power compensator to precisely track the reactive power of the load.

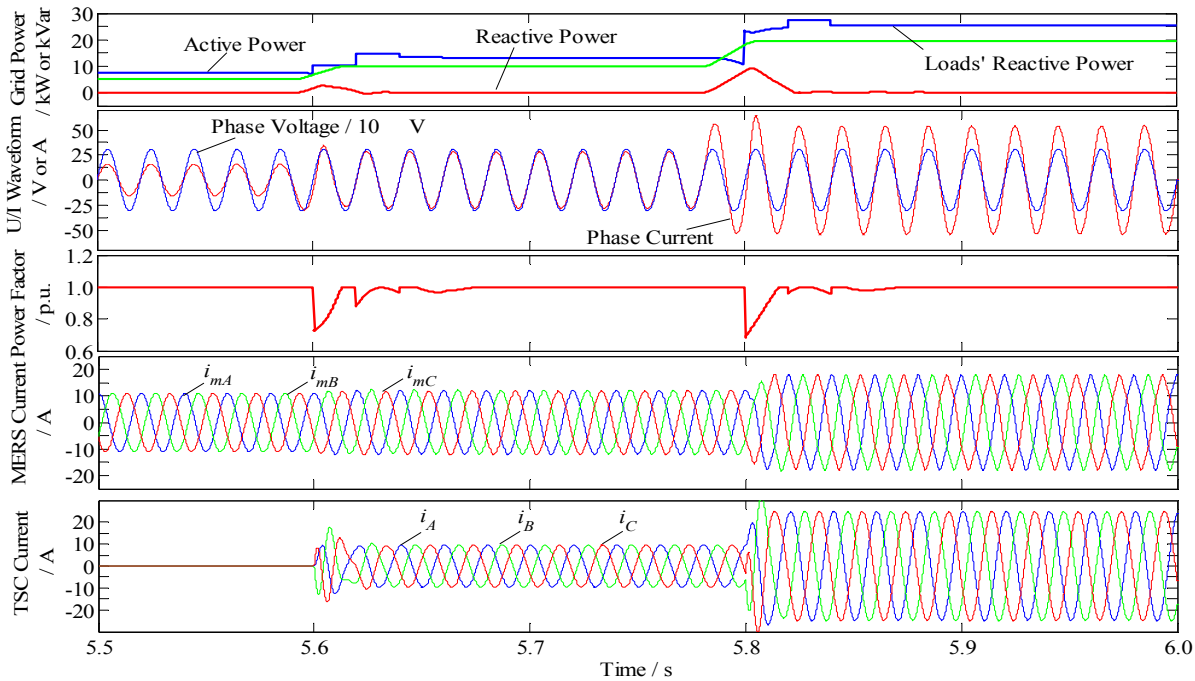

Fig. 12.Response characteristics when Q_{out}increases.

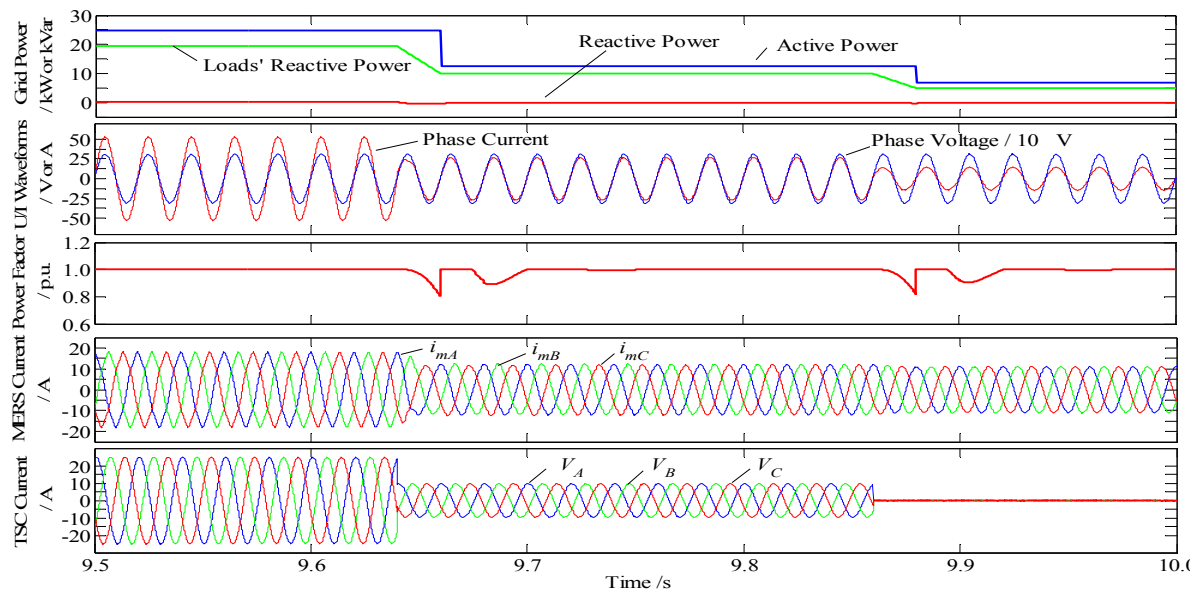

Fig. 13.Response characteristics when Q_{out} decreases.

Using the evaluation model proposed in equation (12), we test the distribution of the optimal working points through simulation (Fig. 14). The points of the same color have the same value of F. Fig. 14 shows the variation tendency of F, which aids in determining the best working point.

(2) Experiment verification: With MERS and TSCs, a continuous and wide-ranging reactive power is supplied to maintain the balance of the grid power. The experimental results verify this feature in practical applications (Fig. 15). Before the load increases, the power grid reaches a balance, as shown in Fig. 15(a). The connected TSC_1 and MER generate the same reactive power needed by the load. TSC_2 is also switched in the grid a few moments after the load increases at 0.9 s. MERS starts to regulate the power factor at the same time. Point A is in a state when the balance of the grid is restored. TSC_1 is cut off from the grid because the load decreases at 5.3 s. The system returns to normal quickly. Point B is in a state when the balance of the grid is restored. Fig. 15(b) shows the phase voltage and current waveforms of the grid at points A and B. Fig. 15(c) shows the MERS capacitor voltage and current of these two points. Finally, the power factor is corrected to a value higher than 0.95.

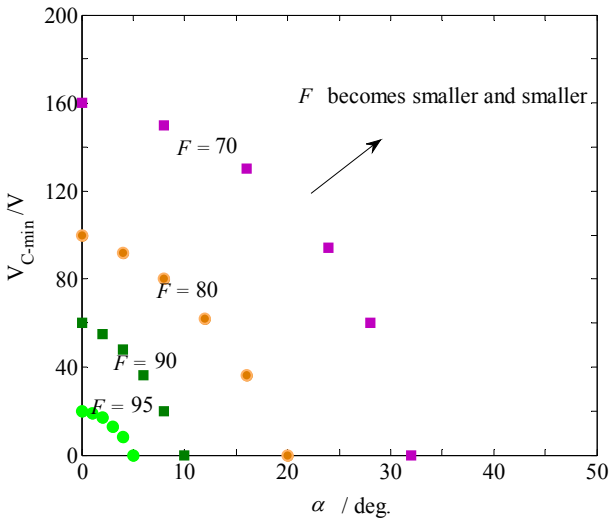

Fig. 14.Performance of working points measured by simulation.

Using the novel continuous reactive power compensator, we also test its steady-state performance and present the result in Fig. 16.The improvement of the power factor with a continuously increasing load is concluded by comparing the cases with and without MERS. The power factors simulated in the computer are also measured and presented in Fig. 16 as a reference.

C. Comparison with STATCOMs

The feasibility of the proposed switch as a novel continuous reactive power compensator is verified. Compared with STATCOMs, the parallel-connected MERS offers more remarkable advantages.

1) Low Losses

Although a three-phase MERS comprises two more switches relative to STATCOMs, the numbers of switches of the two systems operating at any given time are the same. For a

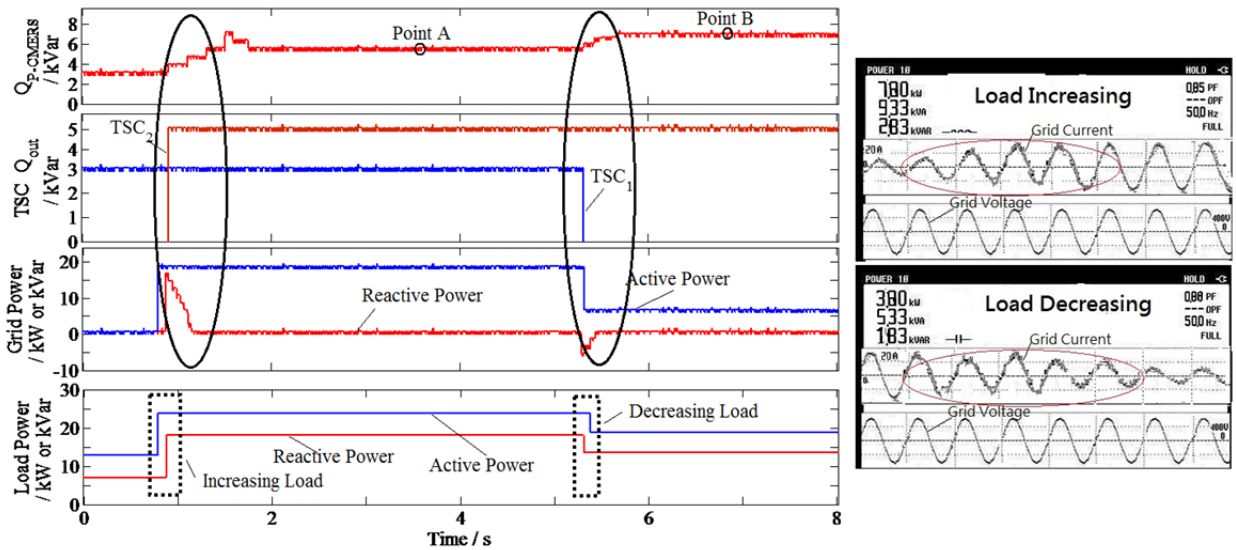

(a) Transient response for power balance.

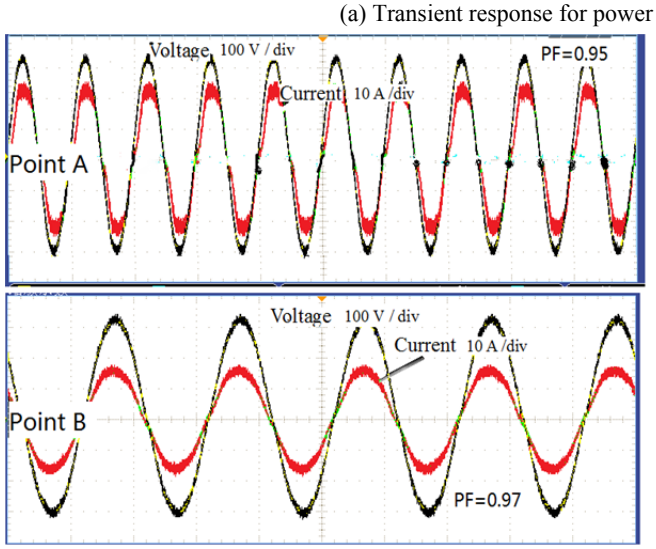

(b) Grid voltage and current.

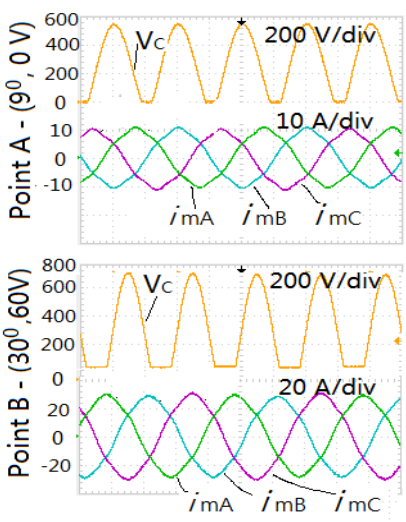

(c) V_C and MERS current.

Fig. 15.Experimental results for power factor correction.

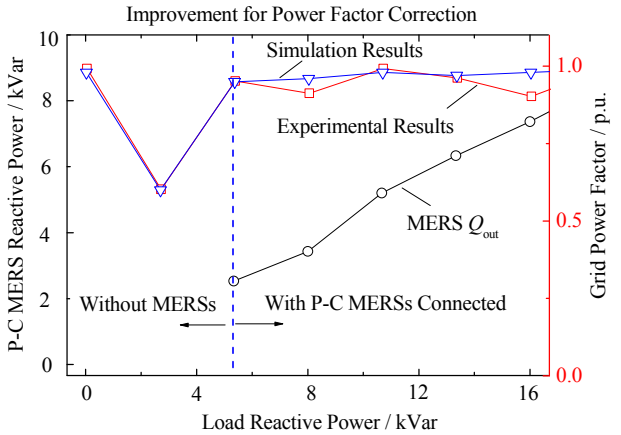

Fig. 16. Steady-state performance for power factor correction.

triangle-connected three-phase MERS, each phase voltage is higher than that for STATCOMs. Therefore, the phase current of a STATCOM is larger than that of the proposed compensator when they work in the same conditions and supply the same reactive power. Thus, a STATCOM experiences more conduction loss than the proposed device on each IGBT. Moreover, the high-frequency control for a STATCOM leads to considerable switching losses.

2) Small DC Capacitor

A dc capacitor is adopted for the shunt MERS and STATCOM. Even though three capacitors are installed in the three-phase system, the size of the dc capacitor of the system is several times smaller than that of a STATCOM. Furthermore, its equivalent capacitance is controllable and tends to increase with increasing α.

3) Easy to Control

The developed control method is based on the phase-delay control. The generation of driven signals under this method is simple because of the absence of complex calculations or coordinate transformations. In addition, every phase of the proposed MERS can be regulated separately.

V. Conclusions

A novel type of SVC called MERS is investigated. In the theoretical analysis, MERS is first introduced, along with its circuit configuration, operating principle, and mathematical model. To improve the effect of reactive power compensation, we propose a new control method for this device to restrain current harmonics and the peak voltages of capacitors. Then, this control method is tested through simulations and experiments. The new compensator is also compared with a STATCOM. The feasibility and advantages of the shunt MERS as an emerging reactive power controller are finally verified.

References

[1] J. A. Barrado, R. Griñó, and H. Vald-Blavi, "Power-quality improvement of a stand-alone induction generator using a STATCOM with battery energy storage system," *IEEE Trans. Power Del.*, Vol. 25, No. 4, pp. 2734-2741, Oct. 2010.

[2] L. Spasojević, I. Papič, and B. Blažič, "Development of a control algorithm for a static VAR compensator used in industrial networks," *Journal of Power Electronics*, Vol. 14, No. 4, pp. 754-763, Jul. 2014.

[3] B. Singh, S.S. Murthy, and S. Gupta, "STATCOM-based voltage regulator for self-excited induction generator feeding nonlinear loads," *IEEE Trans. Ind. Electron.*, Vol. 53, No. 5, pp. 1437-1452, Oct. 2006.

[4] F. D. Wijaya, T. Isobe, K. Usuki, and J. A. Wiik, "A new automatic voltage regulator of self-excited induction generator using SVC magnetic energy recovery switch (MERS),"in *IEEE Power Electronics Specialists Conference*, pp. 697-703, Jun. 2008.

[5] M. S. El-Moursi and A. M. Sharaf, "Novel controllers for the 48-pulse VSC STATCOM and SSSC for voltage regulation and reactive power compensation," *IEEE Trans. Power Syst.*, Vol. 20, No. 4, pp. 1985-1997, Nov. 2005.

[6] B. Singh, S. S. Murthyand, and S. Gupta, "Analysis and design of STATCOM-based voltage regulator for self-excited induction generators," *IEEE Trans. Energy Convers.*, Vol. 19, No. 4, pp. 783-790, Dec. 2004.

[7] R. K. Varma, S. A. Rahman, and T. Vanderheide, "New control of PV solar farm as STATCOM(PV-STATCOM) for increasing grid power transmission limits during night and day," *IEEE Trans. Power Del.*, Vol. 30, No. 2, pp.755-764, Apr. 2015.

[8] B. Gultekin and M. Ermis, "Cascaded multilevel converter-based transmission STATCOM: system design methodology and development of a 12 kV ±12 MVAr power stage," *IEEE Trans. Power Electron.*, Vol. 28, No. 11, pp.4930-4950, Nov. 2013.

[9] M. M. Cheng, K. Feng, T. Isobe, and R. Shimada, "Characteristics of the magnetic energy recovery switch as a static Var compensator technology," *IET Power Electronics*, Vol.8, No.8, pp.1329-1338, Aug. 2015.

[10] Y. Wei, L. Kang, Z. Huang, Z. Li, and M. M. Cheng, "A magnetic energy recovery switch based terminal voltage regulator for the three-phase self-excited induction generators in renewable energy systems," *Journal of Power Electronics*, Vol. 15, No. 5, pp.1305-1317, Sep. 2015.

[11] J.A. Wiik, O. J. Fonstelien, and R. Shimada, "A MERS type series FACTS controller for low voltage ride through of induction generators in wind farms," in*13th European Conference on Power Electronics and Applications*, pp. 1-10, Sep. 2009.

[12] T. Kawaguchi, T. Sakazaki, T. Isobe, and R. Shimada, "Offshore windfarm configuration using diode rectifier with MERS in current link topology," *IEEE Trans. Ind. Electron.*, Vol. 60, No. 7, pp. 2930-2937, Jul. 2013.

[13] M.M. Cheng, D. Shiojima, T. Isobe, and R. Shimada, "Voltage control of induction generator powered distributed system using a new reactive power compensator SVC-MERS," in*15th International Power Electronics and Motion Control Conference (EPE/PEMC)*, pp. 71-78, Sep. 2012.

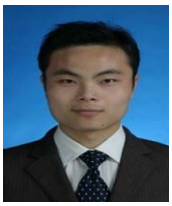

Yewen Wei was born in Hunan province, China. He received his B.S. degree in Measurement and Control Technology for Instruments from Xiangtan University, Xiangtan, China, in 2008, and his Ph.D. degree in Power Electronics and Power Drives from the School of Electric Power, South China University of Technology, Guangzhou, China, in 2015. His current research interests include power electronic converters, the application of power electronics in renewable energy systems, reactive power control, harmonics, and power quality compensation systems, such as SVC, magnetic energy recovery switch (MERS), and FACTS devices.

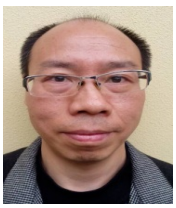

Bo Fang was born in Henan province, China. He received his B.S. degree in College of Automation & Information from Xian University of Technology, Xi'an, China, in 2006. His current research intere sts include power electronic converters, the application of power electronics in renewable energy systems, reactive power control, harmonics, and power quality compensation systems, such as SVC, magnetic energy recovery switch (MERS)

Longyun Kang was born in Jilin, China, in 1961. He received his B.S. degree in Physics from Yanbian University, China, in 1982, and his M.S. and Ph.D. degrees in Electrical Engineering from the Engineering Department of Kyoto University, Japan, in 1996 and 1999, respectively. From 1999 to 2001, he was a Researcher with the Department of Engineering, Tokyo Institute of Technology. From 2001 to 2006, he was an Associate Professor with the Institute of Mechanical Engineering, Xi'an Jiaotong University. Since 2006, he has been with the School of Electric Power, South China University of Technology, where he is currently a Professor. He supervises a Ph.D. student and serves as a Director of Guangdong Key Laboratory of Clean Energy Technology. His current research interests lie in the area of renewable energy and electric vehicles, including wind energy, solar energy conversion, hybrid energy systems, and hybrid-drive technology of electric vehicles.

Zhizhen Huang was born in Anhui, China, in 1990. He received his B.S. degree from Xiangtan University, Xiangtan, China, in 2013. Since 2013, he has been working toward his M.S. degree in the School of Electric Power, South China University of Technology, Guangzhou, China. His current research interests include power electronic converters and vehicle wireless charging technology based on MERS.

Teguo Liu was born in Hunan province, China. He received his B.S. degree in Mathematics and Applied Mathematics from Hunan University of science and Technology, Xiangtan, China, in 2004, and his Ph.D. degree in high voltage and electrical insulation from the School of Electric Power, South China University of Technology, Guangzhou, China, in 2014. His current research interests include electrical insulation, reactive power control, harmonics, and power quality compensation systems, such as SVC, and FACTS devices.